



# The Caravel heX-Mesh pavilion, illustration of a new strategy for gridshell rationalization

Xavier Tellier<sup>1,2</sup> · Sonia Zerhouni<sup>3</sup> · Guillaume Jami<sup>3</sup> · Alexandre Le Pavéc<sup>3</sup> · Thibault Lenart<sup>3</sup> · Mathieu Lerouge<sup>1</sup> · Nicolas Leduc<sup>1,3</sup> · Cyril Douthe<sup>1</sup> · Laurent Hauswirth<sup>2</sup> · Olivier Baverel<sup>1,4</sup>

Received: 5 December 2019 / Accepted: 17 March 2020 / Published online: 31 March 2020  
© Springer Nature Switzerland AG 2020

## Abstract

The fabrication of a freeform structural envelope is usually a highly complex task. The costliest aspect is often the connections between the constitutive parts. The Caravel heX-Mesh Pavilion is a prototype that demonstrates a new rationalization strategy. Its structure, composed of a hexagonal grid of beams and cladding panels, is based on a geometry that rationalizes connections at two levels. Firstly, nodes are free of geometrical torsion and are repetitive: only two types of nodes are used. Secondly, panels can easily be connected to the support beams as they are orthogonal to each other. The mechanical behavior is validated by finite-element analysis. We generate these meshes by numerical optimization from a smooth target surface, with an initialization derived from the asymptotic case and surface theory. The pavilion shows an alternative way of rationalizing a gridshell beyond the popular planar-quad meshes and circular/conical meshes. It also demonstrates a way to generate hexagonal gridshells which are not necessarily synclastic, this limitation being typically imposed to achieve planarity of cladding panels.

**Keywords** Architectural geometry · Gridshell · Hexagonal mesh · Free-form surface · Rationalization · Pavilion · Node repetition

## 1 Introduction

Free-form architectural structural envelopes have become increasingly popular in the past decades. The cost of these projects is usually strongly impacted by the fabrication of the nodes, which often need to be all unique. The connection between beams and panels is also problematic, as the kink angles between adjacent panels often vary significantly.

Two main geometrical strategies have been studied and used to simplify node fabrications in order to reduce their cost. The first one is to use a geometry that allows for torsion-free nodes. In such nodes, all the median planes of the incoming beams meet on a common axis. This

property can be achieved by having all beams in a vertical plane or by using circular or conical meshes [1, 2]. Planar hexagonal meshes also have torsion-free nodes, but the hexagons are necessarily non-convex (shaped like a bow-tie) in anti-clastic surfaces [3].

The second one is node repetition. As detailed by Eike Schling in [4], node repetition can be achieved by two means. The first one is to have the exact same geometry for each node, or for some groups of nodes. For example, this can be achieved with meshes of revolution, or with isogonal molding surfaces [5]. The second one is to use construction tolerances or adjustable nodes to allow one or more degrees of angle variation with a same physical

✉ Xavier Tellier, [Xavier.tellier@enpc.fr](mailto:Xavier.tellier@enpc.fr) | <sup>1</sup>Laboratoire Navier, UMR8205, Ecole des Ponts, UGE, CNRS, Champs-sur-Marne, France. <sup>2</sup>Laboratoire d'Analyse et de Mathématiques Appliquées, UMR8050, UGE, Champs-sur-Marne, France. <sup>3</sup>ENS Architecture Paris Malaquais, Paris, France. <sup>4</sup>GSA/ENS Architecture, Grenoble, France.



connector. This last option was for example used in the Neckarsulm swimming pool dome [6].

One could then name a third aspect that is very important for the detailing of façade: the beam-panel connection. Indeed the variation of the kink angle between the panel and the top surface of the beams renders impossible to make the connection structural, and thus to use the cladding system as a structural element. Furthermore, complex joining systems are needed if the kink angle is too high and sealing becomes hard to achieve. The optimization for a structural layout regarding the kink angle between beam and panel was hence at the starting point of the thought on Caravel meshes which were first presented in [7], extended in [8] and give birth to the Caravel Pavilion shown in Fig. 1.

In this article, we propose a new geometric configuration, based on a hexagonal mesh, which solves the three issues. In Sect. 2, we detail this geometric structure, discuss its potential applications, and prove its existence. A generation method is then presented in Sect. 3. Finally, in Sect. 4, we present how this process has been applied to design and rationalize the Caravel pavilion.

## 2 A new torsion free geometrical configuration

### 2.1 Caravel meshes

The proposed geometrical configuration is a continuation of the work presented in [7], and is shown in Fig. 2. The configuration is based on a hexagonal mesh with non-planar faces. Each of its nodes is assigned with an axis. The configuration satisfies the following properties:

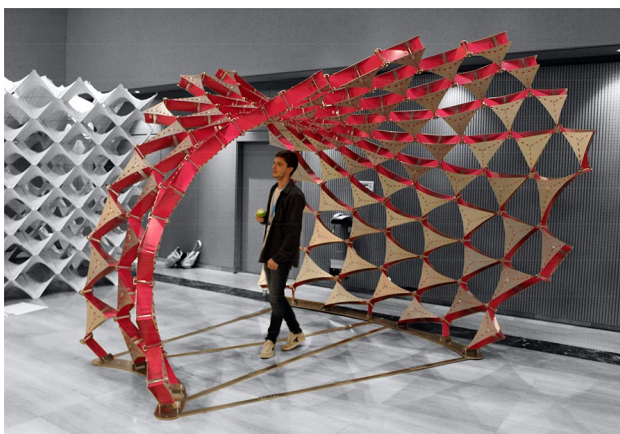


Fig. 1 Three quarter view of the pavilion built for the IASS symposium in Barcelona, 2019

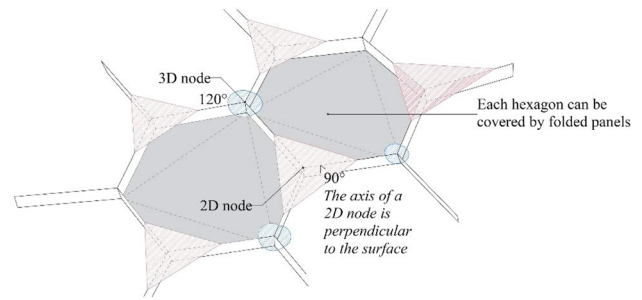


Fig. 2 Geometrical configuration

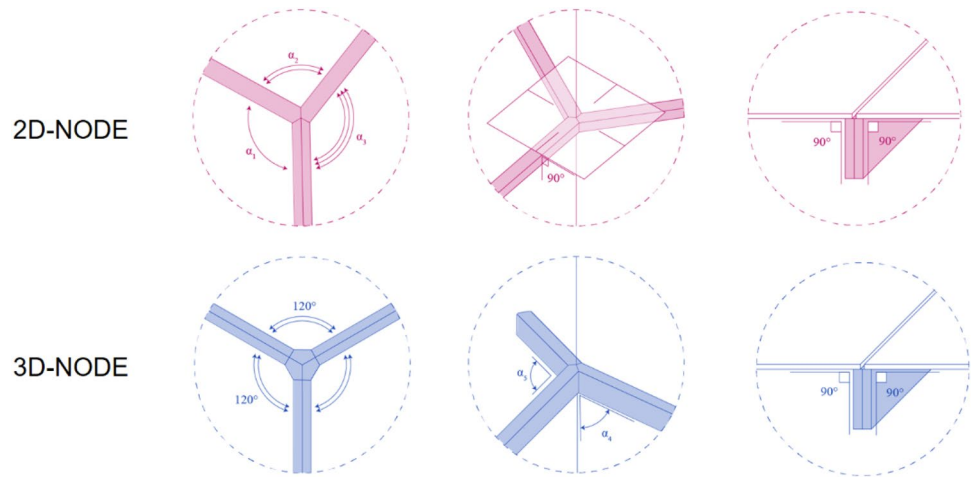
- (a) The axes of two adjacent nodes are coplanar and their common plane corresponds to the median plane of the beam;
- (b) Every other node is flat: the incoming edges are coplanar. These nodes are referred to as 2D nodes, the other nodes are named 3D nodes;
- (c) For 2D nodes, the axis is perpendicular to the plane of the node;
- (d) For 3D nodes, the beam planes intersect at 120°.

This mesh can be used to design a hexagonal gridshell covered by tri-folded hexagonal panels. In that case, the properties that we just described can significantly simplify the fabrication, in particular with respect to the connections between the structural elements, as shown in Fig. 3. Firstly, the contact between panels and beams top surface is perfect and the angle between beam webs and panels is 90°. Thanks to these properties, standard low-cost connections can be used to structurally connect beams to panels. Secondly each node is torsion-free: medial axes of beams meet on a common axis. As a result, structural depth can easily be given to the grid. Thirdly, one half of the nodes are planar, and for the other half, beam planes intersect at 120°, thus allowing a standardization of all beam connections.

The thus formed gridshell is a cladded honeycomb structure. We note that Jiang et al. [9] proposed a method to design this type of structure without torsion on an arbitrary target surface. However, they do not constrain the node axes to be normal to the surface. This is major difference with our configuration, which is therefore much more constrained geometrically.

The proposed properties (a) (b) and (c) form a new type of geometrical structure, based on a mesh in which face normals and vertex normals are coplanar. The proposed application is based on a hexagonal pattern, but many other types of patterns and structural applications are possible [7, 8]. For clarity, we propose to name this type of mesh a *Caravel mesh*, a name which invites to explore *meshes with CoplanAR fAce and VERtEx normals*.

**Fig. 3** Geometry of connections structural elements



**2.2 Asymptotic existence on any smooth surface**

In [8], we prove by construction the existence of the geometric structure described in the previous sections in the asymptotic case, i.e. in the case where a mesh approximates a surface with smaller and smaller face size. In this case, properties can then be described in the setting of smooth differential geometry. It can be shown that it is asymptotically possible to construct our geometry from a planar hexagonal mesh approximating a smooth surface *S* without umbilics and such that one family of hexagon edges is aligned with curvature directions.

Let us start by introducing a classical local approximation model of a surface. A surface *S* can be locally approximated at any point *P* at the second order by a paraboloid. This paraboloid is elliptic if the Gaussian curvature *K* is positive (i.e. the surface is synclastic), cylindrical if *K*=0, and hyperbolic if *K*<0 (i.e. the surface is anticlastic). The equation of this paraboloid is, in the tangent plane at *P*:

$$z = \frac{1}{2}(k_1x^2 + k_2y^2)$$

where *k*<sub>1</sub> and *k*<sub>2</sub> are the principal curvatures. The unit normal of the paraboloid at a point (*x,y,z*) neighboring *P* is given by:

$$\vec{n}(x,y) = n(x,y)(-k_1x; -k_2y; 1)$$

The application (*x,y*) →  $\vec{n}(x,y)$  is referred to as the surface Gauss map. The value of the real factor *n*(*x,y*) will not be important here. Considering a neighborhood such that  $|x| \ll 1/k_1$  and  $|y| \ll 1/k_2$ ,  $\vec{n}(x,y)$  belongs at the first order to a horizontal plane, and is then an orthotropic dilatation in the directions *x* and *y*. The ratios of the dilatation in the *x* and *y* directions are *k*<sub>1</sub> and *k*<sub>2</sub>, up to an homothety (the scaling of the Gauss map is not important in our construction).

After this preliminary considerations, we are now going to construct a mesh and its vertex normals satisfying the properties described in the previous sections. We will use a capital *N* to describe the mesh normals, as they often differ from the surface normals *n*.

Let us first consider a series of planar hexagonal meshes with decreasing faces sizes approximating *S*, and with one family of edges aligned with a principal curvature direction. As mesh size tends towards zero, each hexagon tends to have central symmetry and to be inscribed in a homothetic copy of the Dupin indicatrix, as explained in [10] —the Dupin indicatrix being the conic resulting from the intersection between the paraboloid and the plane *z* = 1. As shown in Fig. 4 (left), the surface Gauss map of the Dupin indicatrix is also a conic, with equation  $\frac{x^2}{k_1} + \frac{y^2}{k_2} = 1$  (up to a homothety).

Let us choose an hexagon ABCDEF in Dupin ellipse with AB and DE aligned with the principal direction (i.e. with the axes of Dupin ellipse) and pick three vertices to form a triangle ACE. We build the Fermat center *P* of ACE, i.e. the point such that  $(\vec{PA}, \vec{PC}) = (\vec{PC}, \vec{PE}) = (\vec{PE}, \vec{PA}) = 120^\circ$ . *P* will be a flat node of the mesh, and A, C and E will be 3D nodes. AP, CP, and EP will correspond to beams. Since adjacent hexagons are congruent in the limit case, the angles between beams at E is also 120°. Therefore this construction yields properties (b) and (d).

In order to fulfill property (b), the mesh normal at *P*, *N*<sub>*P*</sub> must be the normal of triangle ABC. This normal is, in the space of normals, the center of the Gauss map of the Dupin indicatrix. As we want no torsion along PA, PE and PC (property (a)), the mesh normal at A, *N*<sub>*A*</sub>, must lie on a line *l*<sub>*A*</sub> parallel to (AP) passing through *N*<sub>*P*</sub>. In the general case, this line does not include the surface Gauss map at A, therefore *N*<sub>*A*</sub> ≠ *n*<sub>*a*</sub> (this is a second order difference, as the normals are equal at the limit).

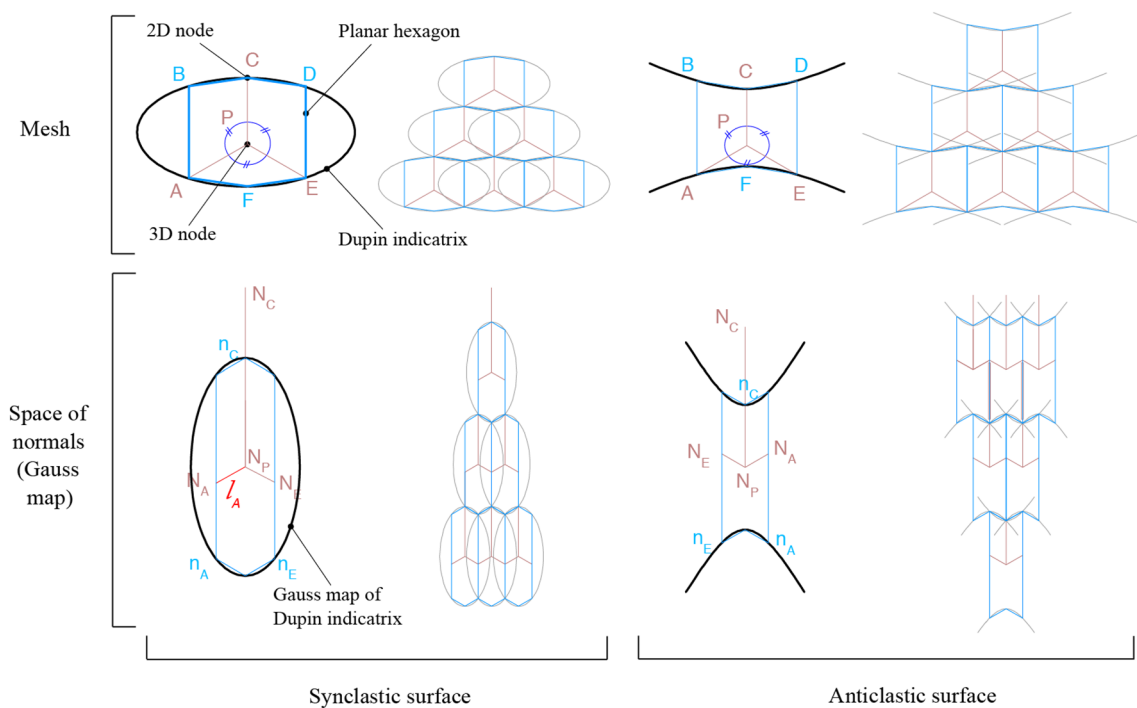


Fig. 4 Asymptotic construction

Now, considering adjacent hexagons Fig. 4 (middle), we observe that the lines previously built intersect at one point with the same lines from the neighboring hexagons if and only if edges AB and DE are aligned with a principal direction (i.e. parallel to an axis of the conic). These intersections points  $N_{Q1}, N_{Q2} \dots$  are the normals of the 3D nodes.

The hexagonal network (in red) along with the attached normals described by the hexagonal mesh on the Gauss map (also in red) verify all the geometrical properties described in the previous sections.

### 3 Generation method

We now give a method to generate the geometrical configuration described in Sect. 2. In a first step, we compute an initial mesh close to this configuration. In a second step, we optimize node position and normals orientation such that properties (a) to (d) are satisfied within given tolerances.

#### 3.1 Mesh initialization

The designer starts hence by defining a target geometry, in the present case a channel like smooth surface (see Fig. 5i). The surface is then meshed by its principal curvature lines (see Fig. 5ii). One then chooses one of the two

principal directions to build a two-colorable triangular mesh on the surface picking out one out of two nodes of the curvature network (see Fig. 5iii). The nodes of this triangular mesh are the future 3D-nodes of the caravel mesh. After what, the Fermat points of one half of the triangular faces (the colored ones in Fig. 5iii) are constructed. Those nodes are planar and will be the future 2D-nodes of the caravel mesh. Connecting finally 2D-nodes and 3D-nodes, one gets a hexagonal mesh, aligned with principal curvature directions where one out of two nodes is planar (see Fig. 5iv). One needs then to assign a normal to each node. By default one chooses the normal to the triangular faces for the 2D-nodes and the normal to the surface for the 3D-nodes.

#### 3.2 Geometrical optimization

Based on the asymptotic analysis, this mesh and its oriented normals is close to a Caravel mesh, but it does not fulfill the properties (a) to (d) exactly yet. To meet those properties, an optimization is necessary.

A non-linear optimization is conducted within the framework of Rhinoceros®'s plugin Kangaroo2. The underlying algorithm is made of multiple geometrical criteria which are expressed as a projection [11]. The first criterion forces every node of valence three to be torsion-free (property (a)), by requiring the normals of the three neighboring nodes to be such that the median planes of the beams



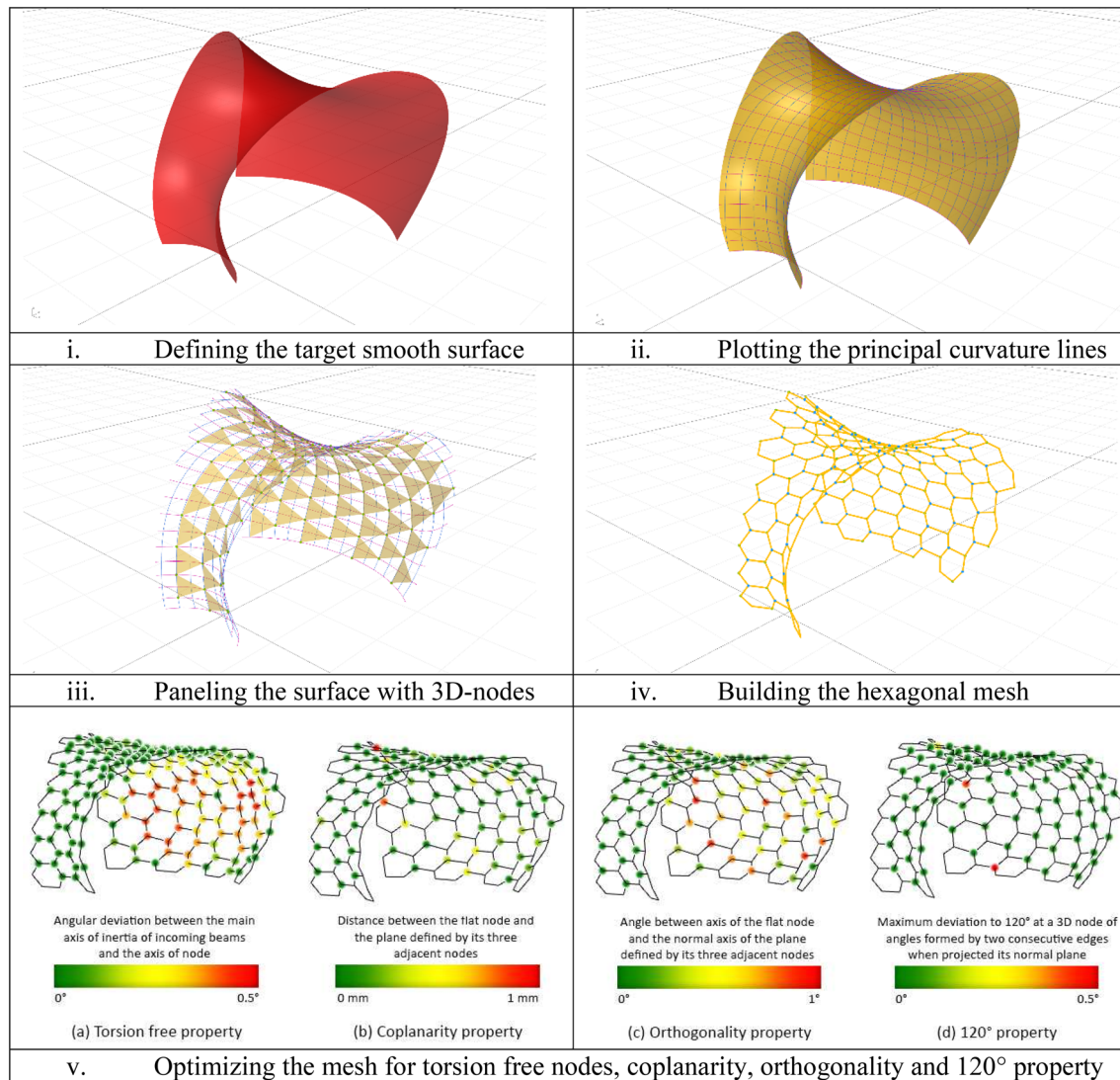


**Fig. 5** Shape generation method for the Caravel Pavilion, from smooth Surface to optimized mesh

coming to the node meet on a common line corresponding to its normal. The second criterion makes the 2D nodes and their respective neighboring nodes coplanar (property (b)). The third one constraints the normals of the 2D nodes to be respectively aligned with the normals of the planes defined by their three neighboring nodes (property (c)). Finally, the fourth one forces 3D nodes to be, when projected on the triangles defined by their three neighboring nodes, the Fermat points of these triangles (property (d)). Complementary criteria are also set for smoothing purposes, such as proximity to the target surface, and to treat the boundaries.

This optimization problem is highly non-linear and non-convex. Hence, there is no theoretical guarantee that the mesh obtained after iterations of the optimization algorithm perfectly meets all the criteria or reach a

global minimum of the problem. However, empirically, the resulting mesh tends to satisfy all the geometrical properties within very low tolerances as shown in Fig. 5v:

- less than  $0.5^\circ$  for torsion angle at nodes (a),
- less than 1 mm for planarity default at 2D-nodes (b), for member sizes around 500 mm in the Caravel Pavilion case,
- less than  $1^\circ$  distortion between panel normal and beam normals (c) and
- less than  $0.5^\circ$  tolerance on the  $120^\circ$  intersections between beam planes on 3D-nodes (d).

Thus, this two-step method (initialization-optimization) allows in practice to generate a geometrical configuration as described in Sect. 2 within acceptable tolerances.

### 3.3 Comparison with other hexagonal meshing methods

There exist many other methods to generate hexagonal meshes with different geometrical properties. In architecture, the generation of hexagonal meshes with planar faces has raised a lot of attention [3, 10, 12, 13]. A major limitation of planar hexagon meshes is that they have non-convex faces when curvature is negative [14], p 705, which is not the case with Caravel meshes. Planar hexagonal meshes are preferably aligned with curvature directions to avoid skewed faces [15]. The proposed method then yields the same distribution and size of faces, except that faces are always convex.

Other popular methods to generate meshes with mostly hexagonal faces include Voronoi meshes [16, 17], methods based on duals of triangular meshes [12], and subdivision schemes [18]. However, they often yield unstructured meshes, and they offer a poor control of edge orientation, which is critical in the present approach. They also do not offer the Caravel properties.

## 4 The X-Mesh pavilion

In order to demonstrate the innovation and the adaptability of the workflow hereby presented, it was applied to the design and realization of a pavilion for the IASS 2019 Pavilion contest.

### 4.1 Design

The shape of the pavilion is a doubly curved envelope, of which transversal sections are horseshoe arches. The shape has both synclastic and anticlastic portions, as shown in Fig. 6, and demonstrates the ability of our method to generate structures on a broad class of forms. The pavilion is high enough to walk under (see Fig. 6).

The starting point of the design is a horseshoe arch surface, chosen for its aesthetic and its functionality relatively to the implantation site at the IASS exhibition. Such shape cannot be funicular. It therefore highlights the potential of the proposed constructive system to resist bending. Bending stiffness and resistance is allowed by the structural depth of the structure. Usually, structural depth in gridshells amplifies fabrication issues due to geometrical torsion at nodes. This is not the case with Caravel meshes thanks to their torsion-free nodes.

This surface was discretized by a hexagonal mesh aligned with curvature lines. There are two ways to align a hexagonal mesh with curvature directions. The alignment with the horizontal curvature lines is chosen in order to create the graphic impression of an ascending movement, as the triangular panels are pointing upwards diagonally.

The concept of this pavilion focuses on highlighting the geometrical properties through the architectural treatment of the elements, especially the connections. The conception of each type of node is entirely based on the geometrical rationalization that simplifies its fabrication, and takes advantage of each geometrical strategy to define its technology.

### 4.2 Surface optimization for mesh alignment with ground level

For aesthetic and fabrication reasons, it was desirable to align the mesh with the ground. Since the mesh follows curvature directions, we modified the target surface so that its bottom boundaries (verifying  $z=0$ ) are curvature lines. By the Joachimsthal theorem, this property is achieved if the surface has a constant slope along the lines  $z=0$ . As our target surface is a B-spline, the slope at the ground boundary is given by the bottom two rows of control points. We therefore optimized the position of these control points so that the slope of the surface is constant at the ground level (see Fig. 5ii).

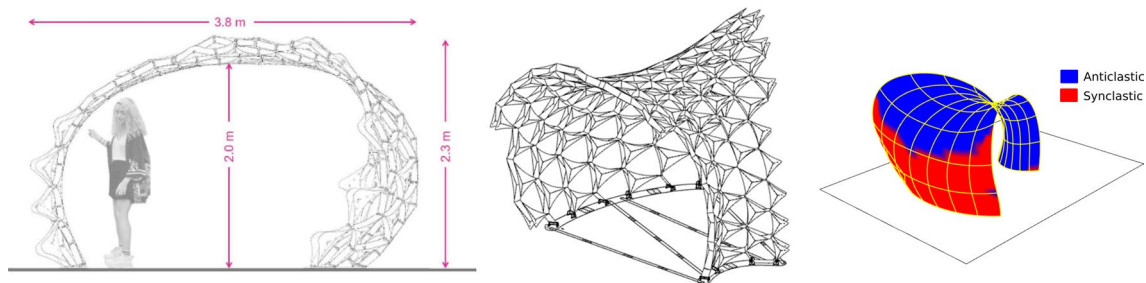


Fig. 6 Shape and dimensions of the Caravel Pavilion

### 4.3 Detailing

#### 4.3.1 Beams

The torsion free nodes allowed us to conceive the main hexagonal grid as a beam structure. Indeed, since adjacent node axes are coplanar, their common plane defines the median planes of beams. This allowed to build all elements out of sheet materials. After structural analysis (see Sect. 4.4), it was hence decided to build the hexagonal grid 4 mm thick laser-cut aluminum plates and to

paint them pink to differentiate them from the cladding (see Fig. 1).

#### 4.3.2 Two standard connectors

We took advantage of the node repetition to design two standards types of connections, one for each type of geometrical node (2D and 3D). These nodes are showed in Figs. 7 and 8. 2D nodes (Fig. 7) offered us the possibility to create a structural connection through the common plane of the three incoming beams. This connection was

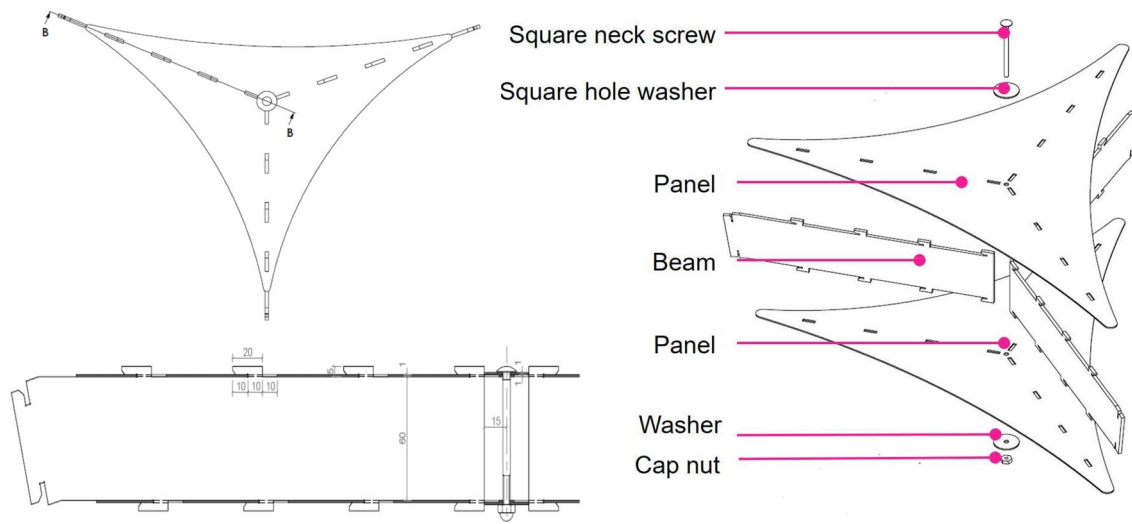


Fig. 7 Technological solution for the 2D nodes

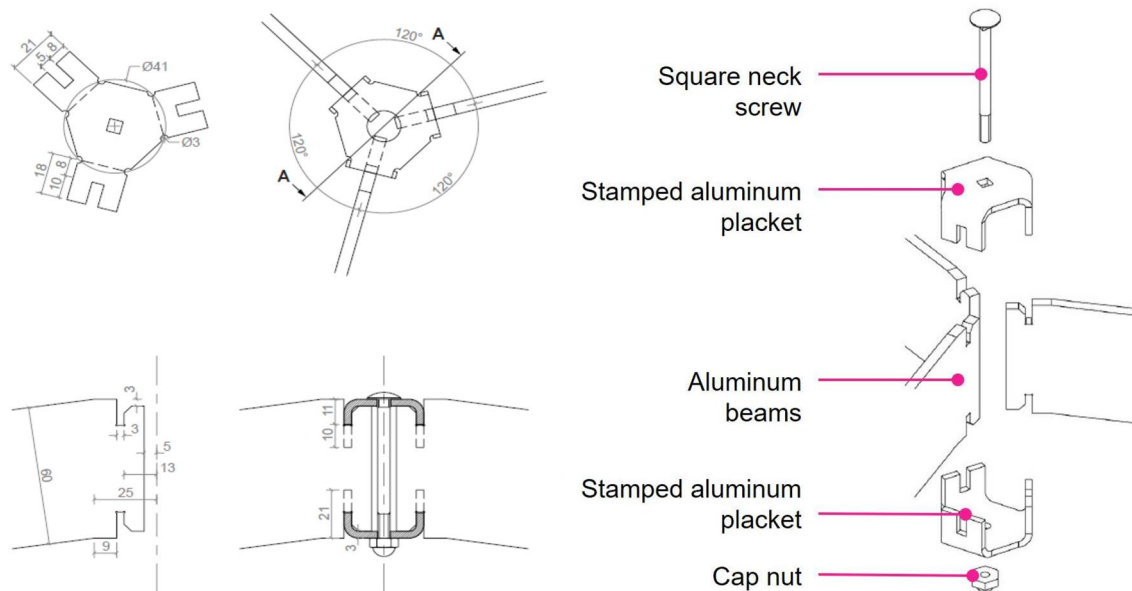


Fig. 8 Technological solution for the 3D nodes

realized by two 1 mm thick galvanized steel panels on the superior and inferior edge of the three beams. Structurally, the height of the beams can be adjusted to have sufficient vertical inertia. The horizontal inertia is guaranteed by the cladding panels. Panels are fixed to the edges of the three beams thanks to locking tabs in which the carved panels are pushed into. As beams are orthogonal to panels, all the cuts are orthogonal to the sheet planes, and can thus be realized by 2D laser cutting.

The technological treatment of the 3D nodes (Fig. 8) is based on the existence of an axis assigned to each node and on the fact that beam planes always intersect at  $120^\circ$ . For 3D nodes, a hinged connection is built from two pieces, cut out from 4 mm aluminum sheets and swaged in a stamping press. These formed parts are all identical and guarantee the  $120^\circ$  angle between each beam plane of the 3D node. They are maintained in place thanks to a single screw, materializing the direction of the normal axis of the node. A lug has been added on every member end as well as corresponding adjusted square holes in the stamped aluminum placket in order to lock the rotation of the beams in the nodes.

#### 4.3.3 Edge details

The two types of junctions are adapted on the free edges of the pavilion; thus it is unnecessary to develop an entirely different solution for the nodes on the boundary (see Fig. 9). Only two beams are joined on 3D nodes on naked edges, so in order to keep the same technological solution, we added a short stub that closes the node. 2D nodes with only two beams can work the same way on naked edges than on interior edges, as long as the panel is designed accordingly. This degree of freedom offers the opportunity to adapt the general design of the edge.

#### 4.3.4 Supports

The pavilion was designed to be autostable so that it does not require ground anchors. Practically, the ground supports are connected between them to form a rigid frame through a floor beam on each side with four ties triangulating the whole, all made of 4 mm thick aluminum plates (see Fig. 6). The supports themselves which are modeled as hinges from a mechanical point of view, are made of two parallel plates slotted into the floor beams that maintain two plates fitting the beam plane and allowing rotation along the desired inclined axes (see Fig. 10). A set of lugs and stops are then designed in order to prevent lifting. This detail can accommodate wide angle variations in two directions, such that it could be used at each of the ten supports. Furthermore, it requires only one bolt to tighten, thus accelerating the assembly and disassembly of the pavilion.

#### 4.4 Structural check

To ensure the safety and structural behavior of the pavilion, we implemented a finite element model of the structure and verified its behavior under dead load and accidental load (0.2kN applied horizontally at 1 m from the ground). The structural check follows then the approach of Eurocode: no damage at ELU and reasonable displacements at ELS (here  $< 4$  cm under the lateral push). The whole pavilion (i.e. beams, panels, basement) is modeled considering hinged supports between structural members and ridge beams of the support (see Fig. 11a). Releases at 2D-nodes and 3D-nodes have then be model carefully:

- At 2D node, the forces and moments are transferred from one beam to the other essentially by the panels.

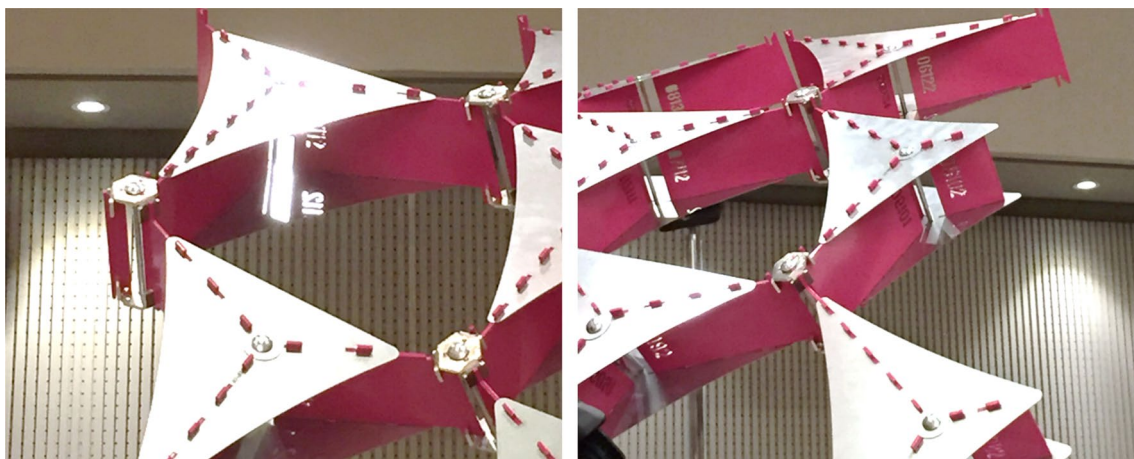
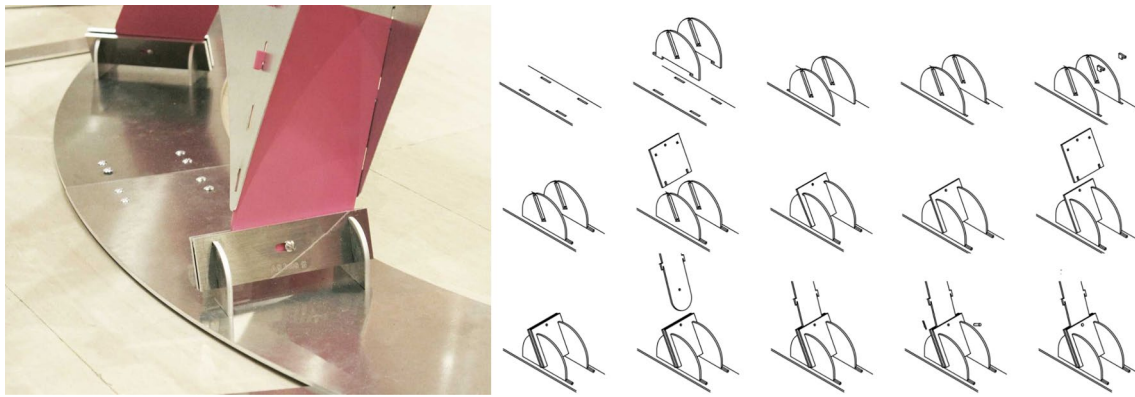


Fig. 9 Free edge treatment 3D node on the left, 2D node on the right





**Fig. 10** Detail of the hinged supports and principle of assembly

Therefore, they have to go through the connectors. In the Caravel Pavilion, these connectors work by contact, through the four L-shaped stops on both top and bottom edges of each beam that slide into corresponding rectangular holes in the panels until they hit one of their edges (see Fig. 7). Holes are accurately cut such that the stops are also laterally in contact with the panels within very low tolerances. For simplicity reasons, the panels are thus represented by sets of galvanized steel *strips* on the top and bottom sides of the beams (1 mm thick and 20 mm wide) as can be seen in Fig. 11a. To connect the strips with the beams neutral axis, rigid links span between the ends of the hinged strips and the beams' axis. Finally considering that the screw/washer system prevents the beams back sliding, relative translations at beams end have been blocked. To account for buckling of the strips, only tension forces are considered in the analyses of the strips.

- At 3D nodes, all forces and moments are transferred through the stamped aluminum plackets which are not perfectly stiff compared to the members. Therefore, a plate finite element model of the placket was used to estimate the stiffness of the connector in the six directions (see Table 1). These stiffness's are then introduced in the global structural model following the local axes of the various members. It appeared that half of the structure displacement comes from the connectors stiffness.

Linear static analyses have then been conducted under gravity load and horizontal push. With the chosen cross sections for the aluminum beams (100 mm height and 4 mm width), the pavilion was found very safe: the maximum stress equals 80% of limit stress, the maximum displacement equals 3.9 cm (2.1 cm vertically) and the eigenfrequency equals 1.7 Hz.

The analysis of displacements (shown in Fig. 11b) reveals that the structure works as an arch defined by a cut along the longitudinal plane YZ. Indeed the displacements are almost equals for all the points on a transversal cut along any plane XZ (except close to the support on the ground where the chosen narrowing is a handicap). The double curvature of the structure ensures thus a certain stiffness in the transversal direction and the transfer of forces from the free edges toward the supports.

This arch behavior is confirmed by the analysis of member forces. When seen from aside the prototype forms a horseshoe arch, which resists forces through a mix of strong axis bending moment  $M_z$  (Fig. 11d) and normal force  $N_x$  (Fig. 11c). The structure is clearly not a funicular shell dominated by membrane forces but still it can be described as a gridshell because all the nodes transfer bending moments along the strong axis giving out-of plane bending stiffness to the structure while the bracing by the panels at the planar nodes gives membrane shear stiffness.

It is worth also remarking that the six directions were solicited. Indeed, due to the hexagonal arrangement of the grid and to the curvature of the global shape, normal forces are transformed into normal forces and shear forces, and bending moments in the strong direction are transformed as well into bending moment in both directions and torsion (see Fig. 11e, f). Despite the low values of these moments, their contribution to the overall compliance of the structure is high. Indeed, the bending stiffness of the strong axis is 500 times higher than the weak axis stiffness and 160 times higher than the torsion stiffness.

It seems hence that for further developments of the Caravel meshes, it will be necessary to investigate the connection between beams and panels so that it can transfer shear and that the system works as an I-beam and change the order of magnitude of the torsional stiffness and weak axis bending stiffness. This could not be

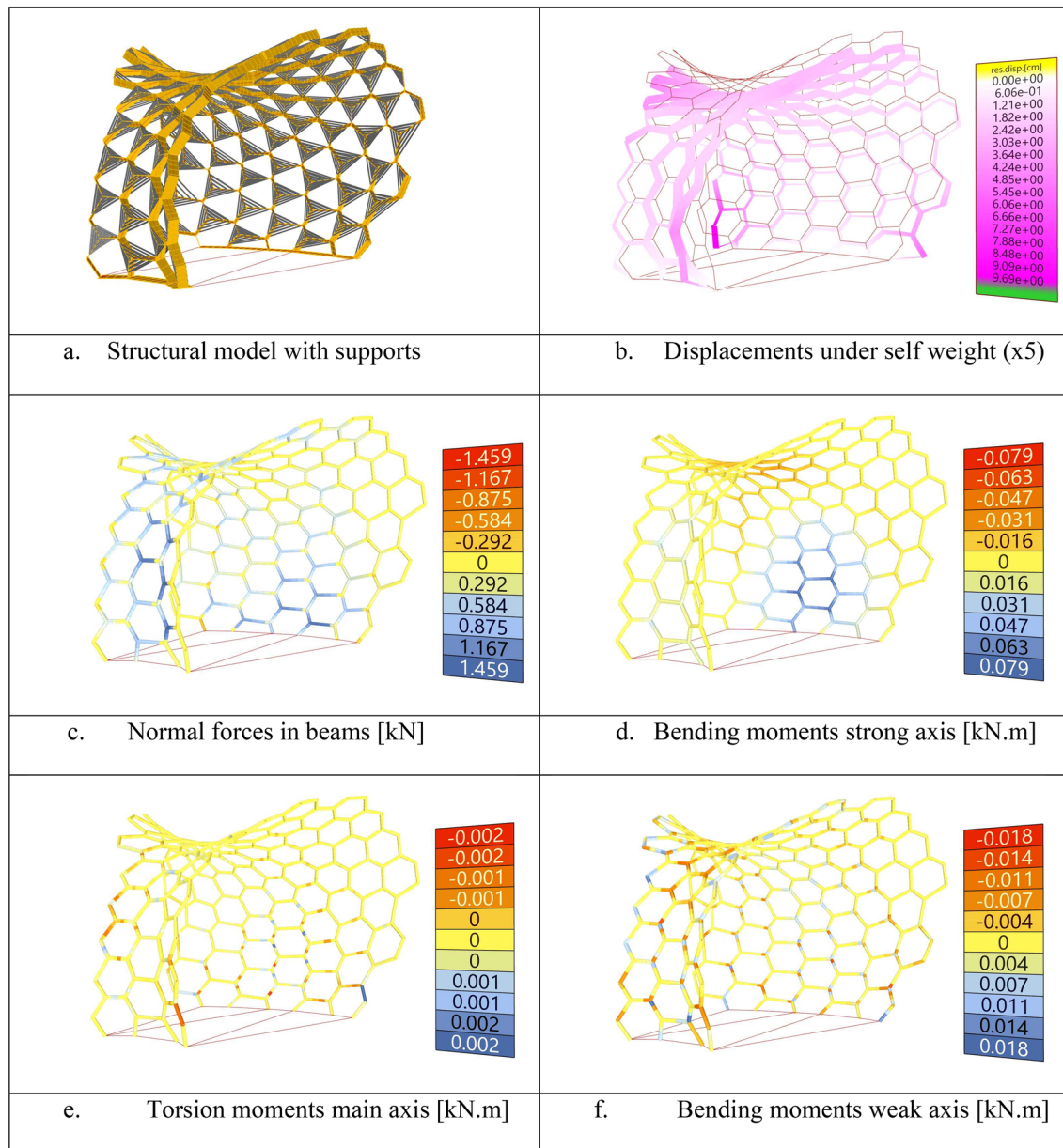


Fig. 11 Structural analysis of the pavilion

**Table 1** Identified characteristics of the 3D-connectors in the member local axes

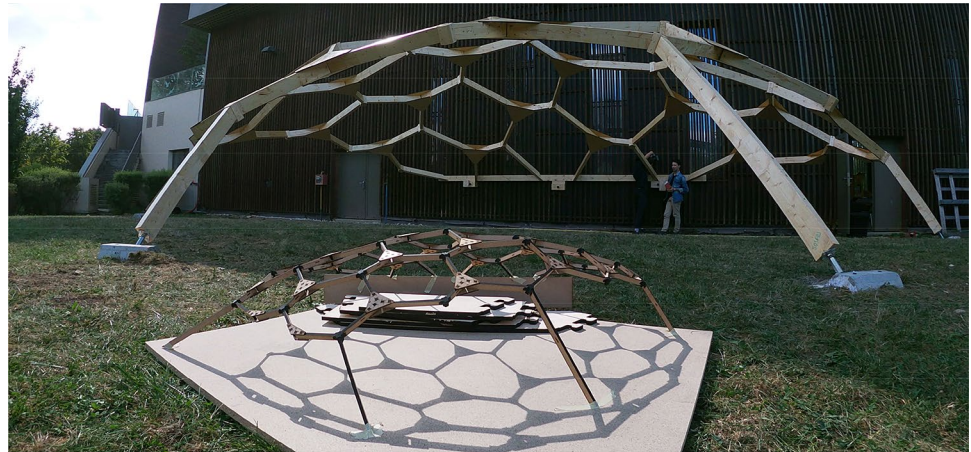
Force	Normal X	Shear Y	Shear Z	Torsion X	Moment Y	Moment Z
Stiffness	21 MN/m	10 MN/m	21 MN/m	25 kNm/rad	25 kNm/rad	∞

done for the presented pavilion which gave priority to assembly methods which were driven here by the fact that the pavilion had to be assembled and disassembled in one day. Besides, it is noticed here that the pavilion was then rebuilt for a three days' exhibition on February 2020 in the main building of the Ecole d'Architecture Paris Malaquais.

### 5 Conclusions

In this article, a new family of meshes combining several rationalization properties was introduced: Caravel meshes. Their potential for structural applications was demonstrated by designing a full scale pavilion which

**Fig. 12** Another application of caravel meshes for a 8 m wooden structure and its 1/10th mockup



was exhibited at the 60th IASS Symposium in October 2019, rebuilt for a temporary exhibition in Paris-Malaquais and will be reassembled a third times for the pavilion exhibition of the “Advances in Architectural Geometry 2020” conference. It was a unique experience of collaboration between mathematics, structural engineering and architecture students and researchers working together on the design of a prototype from differential geometry theory to fabrication. The main issues of the design process of caravel meshes have been tackled: geometric characteristics of caravel meshes, proof of existence on any smooth surface, generation method, structural analysis and detailing. The proposed approach for surface rationalization which only uses two types of nodes (here only two types: 2D flat-node and a 3D 120°-node) seems very promising and opens up a lot of perspectives for innovative design of gridshell structures.

The geometrical and structural principles developed here were meant to be scalable at other structural scale. Indeed from a geometrical point of view, nodal axes of the prototype are clearly identifiable through the bolt axes: the height of the members is a parameter that can be freely adjusted by the designer who can therefore adjust it to the scale and required structural depth. From a technological point of view, the details shown here are adapted to the scale of the prototype and to the fact that it should be dismountable. Should it be built in another context or at another scale, the details should be changed but thanks to the geometrical properties of the structure, those changes are relatively simple or remain in the framework of standard detailing. Two variants of this prototype have indeed been built by the authors: one 8 m span wooden structure and its 1/10 MDF mockup shown in Fig. 12.

**Acknowledgements** The authors would like to thank all funding partners as well as Eike Schling and Daniel Piker for fruitful discussions.

**Funding** The design and fabrication of the Pavilion were financially supported by the I-Site Impulsion grant “Games”, by the Steel contractor VIRY who gently provided the laser-cut panels as well as technical support and by ENSA Paris-Malaquais. This work is also part of the PhD thesis of the first author who is funded by Labex MMCD (<http://mmcd.univ-paris-est.fr/>).

### Compliance with ethical standards

**Conflict of interest** The authors declare that they have no conflict of interest.

### References

- Liu Y, Pottmann H, Wallner J, Yang Y-L, Wang W (2006) Geometric modeling with conical meshes and developable surfaces. *ACM Trans Graph* 25(3):681
- Pottmann H, Wallner J (2008) The focal geometry of circular and conical meshes. *Adv Comput Math* 29(3):249–268
- Wang W, Liu Y, Yan D, Chan B, Ling R, Sun F (2008) Hexagonal meshes with planar faces, HKU CS Technical Report
- Schling E (2018) Repetitive structures. PhD thesis TUM, 2018
- Mesnil R, Douthe C, Baverel O et al (2015) Isogonal moulding surfaces: a family of shapes for high node congruence in free-form structures. *Autom Constr* 59:38–47
- Schalich B and Partners (2019) Freizeitbad aquatoll neckarsulm. <https://www.sbp.de/projekt/freizeitbad-aquatoll-neckarsulm/>. Accessed 13 May 2019
- Tellier X, Baverel O, Douthe C, Hauswirth L (2018) Gridshells without kink angle between beams and cladding panels. In: *Proceedings of IASS symposium 2018 creativity in structural design Boston, USA, 2018*
- Tellier X, Douthe C, Hauswirth L, Baverel O. Caravel meshes: a new mesh family for rationalized design of gridshells (article under review)
- Jiang C, Wang J, Wallner J, Pottmann H (2014) Freeform honeycomb structures. *Comput Gr Forum* 33(5):185–194
- Wang W, Liu Y (2009) “A note on planar hexagonal meshes”, in *nonlinear computational geometry*. Springer, NY, pp 221–233
- Bouaziz S, Deus M, Schwartzburg Y, Weise T, Pauly M (2012) Shape-up: shaping discrete geometry with projections. In: *Eurographics symposium proceedings*

12. Troche C (2008) Planar hexagonal meshes by tangent plane intersection. In: *Advances in architectural geometry*, Vienna, pp 57–60
13. Vaxman A, Ben-chen M (2015) Dupin meshing: a parameterization approach to planar hex-dominant meshing, Technion IIT CS Technical Report
14. Pottmann H, Asperl A, Hofer M, Kilian A (2007) *Architectural geometry*. Bentley Institute Press, Exton, PA
15. Li Y, Liu Y, Wang W (2015) Planar hexagonal meshing for architecture. *IEEE Trans Vis Comput Graph* 21(1):95–106
16. Kunze R, Wolter FE, Rausch T (1997) Geodesic voronoi diagrams on parametric surfaces. In: *Proceedings of computer graphics international conference CGI*, pp 230–237
17. Tonelli D (2014) *Statics aware voronoi grid-shells*. Ph.D. thesis, University of Pisa
18. Claes J, Beets K, Van Reeth F (2002) A corner-cutting scheme for hexagonal subdivision surfaces. In: *Proceedings SMI*, pp 13–20. Shape Modeling International

**Publisher's Note** Springer Nature remains neutral with regard to jurisdictional claims in published maps and institutional affiliations.